Mechanism of Inhibition of Nanoparticle Growth and Phase Transformation by Surface Impurities

Bin Chen,[1,*] Hengzhong Zhang,[1] Benjamin Gilbert,[2] and Jillian F. Banfield[1,2]
[1]*Earth and Planetary Science, University of California–Berkeley, Berkeley, California 94720, USA*
[2]*Earth Science Division, Lawrence Berkeley National Laboratory, Berkeley, California 94720, USA*

(Received 14 October 2006; published 7 March 2007)

Experiments have shown that thermal stability of nanoscale titania is significantly enhanced by the presence of low concentration yttrium dopants, but the mechanism of this effect is unclear. We present extended x-ray fine structure and wide-angle x-ray scattering measurements showing that yttrium is not incorporated in the nanoparticle interior but forms yttrium-oxygen clusters at the nanoparticle surfaces. The surface clusters modify the interfacial free energy, affecting the unit cell parameters, strongly inhibiting nanoparticle growth, and stabilizing the anatase phase up to 700 °C. Molecular dynamics calculations reproduced the experimentally observed Y-O bond lengths in surface yttrium clusters and predict a substantial lowering in anatase surface energy, in agreement with the inferred mechanism for suppression of growth and phase transformation.

DOI: 10.1103/PhysRevLett.98.106103 PACS numbers: 68.03.Cd, 61.10.Ht, 64.70.Nd, 68.47.Jn

Nanoparticles can exhibit distinct properties that may be utilized in development of new materials for catalysis [1] and photovoltaics [2]. In addition to size effects, material properties can be changed by surface environment and impurity, which can alter optical properties [3], coarsening rates, and phase stability [4–6]. Not well understood is the basis for retardation of crystal growth and phase transformation in nanoparticles as the result of addition of impurities that are unlikely to be structurally incorporated. The objective of this study is to explain such effects through study of titania (TiO_2) nanoparticles.

Structurally incorporated impurities have been shown to have systematic effects on the rate of the thermally driven transformation in titania nanoparticles [6–9]. The anatase-to-rutile transformation is slowed when anatase nanoparticles are doped with a cation of valence $> +4$ but favored when the valence $< +4$. Based on these observations, Y^{3+} dopants should promote the anatase-to-rutile transformation. However, prior studies showed that the transformation is inhibited by Y^{3+} impurities [6,7], without explaining this observation. In this study, we performed extended x-ray absorption fine structure (EXAFS) experiments on yttrium-doped titania nanoparticles to determine the local structural environment of Y^{3+} impurities, wide-angle x-ray scattering (WAXS) to investigate the response of titania to the presence of impurities, and molecular dynamics (MD) simulations to understand the structural and energetic consequences of doping.

Titanium oxide typically occurs as one of three polymorphs: anatase, brookite, or rutile [10]. Titanium oxide doped with yttrium was prepared using the sol-gel route in a similar manner to that of Anderson, Gieselmann, and Xu [11], as described by Bischoff [7]. Electron probe microanalyses confirm an Y:Ti atomic ratio of 1.2:100. Annealed samples were produced by heating the raw samples in air for 2 h at the designated temperatures (300–700 °C). X-ray diffraction (XRD) showed that the initial product consists of a mixture of nanocrystalline anatase and brookite, similar to the as-synthesized products of undoped titania.

EXAFS measurements at the Y *K* edge (17300 eV) were made up to $k = 12$ Å^{-1}. The fit results (Table I and Fig. S1 in Ref. [12]) indicate that the Y impurity does not exist as $(Y_xTi)O_{2-3x/2}$; i.e., the Y impurity is not structurally incorporated. This differs from the cases of doping TiO_2 with some other ions (e.g., Cr^{3+} and Fe^{3+}), where impurities are distributed within the nanoparticles [7,8]. The reason why Y^{3+} does not substitute for Ti^{4+} in TiO_2 nanoparticles is very likely the difference in the size of the Y^{3+} (0.892–1.10 Å) and Ti^{4+} ions (0.53–0.605 Å) [13]. Moreover, the first shell scattering in the EXAFS data is well fitted by Y-O bonds of length ~2.3 Å, a nearly 20% mismatch with the Ti-O bond lengths in the nanoparticles (1.92 and 1.96 Å) [14]. For heat-treated nanoparticles, the first shell Y-O coordination number (CN) is six, consistent with the yttrium oxide (Y_2O_3) structure.

TABLE I. Fit results from Y *K*-edge EXAFS of yttrium-doped TiO_2 nanoparticles. Fit ranges: $k = 1$–12 Å^{-1}; $r = 1.2$–2.4 Å. The amplitude reduction factor $So^2 = 0.93$ and the energy shift $\Delta E = -0.68$ eV were obtained from a fit to the reference material, bulk Y_2O_3. Small values of χ^2 indicate good fit figures of merit. σ^2 is the mean squared relative displacement and C_3 the mean cubic relative displacement.

T (°C)	χ^2	CN	R1 (Å)	$\sigma^2(\times 10^{-3}$ Å$^2)$	$C_3(\times 10^{-4}$ Å$^3)$
20	0.060	7.4	2.348	6.955	−6.25
300	0.023	6.3	2.319	11.34	−0.50
400	0.021	5.7	2.322	9.415	−5.48
500	0.022	5.7	2.317	9.975	2.30
600	0.008	5.8	2.298	9.260	−2.73
700	0.590	5.7	2.300	6.030	−0.35

However, the characteristic XRD peaks of Y_2O_3 are not detected from our samples, indicating that, if present, individual clusters of this phase should be smaller than ~1 nm. Furthermore, the Y-O bond length (~2.3 Å) is larger than that of bulk Y_2O_3 (2.2749 Å) [15]. We conclude that yttrium impurities are present mostly as individual, oxygen-coordinated atoms at the titania surface (i.e., as YO_6 groups), and about 15% of the surface oxygen sites are bound to Y [12]. It is impossible to exclude the formation of some multiatom yttrium clusters and, thus, lower effective yttrium surface site coverage. However, the significant property modifications observed suggest that multiatom yttrium clusters should be quite rare relative to single-atom yttrium clusters.

We used MD simulations to investigate the incorporation of yttrium at the surface of anatase nanoparticles at the correct Y : Ti ratio [12]. Figure 1 is a snapshot of the structure of the Y-doped 4 nm anatase nanoparticle. Within the simulation time (63 ps), the Y atoms diffused around the outer surface layer, where they formed surface YO_x clusters ($x = 4$–6) but did not penetrate the nanoparticle interior. The average Y-O bond length is 2.3696 Å, a value that is larger than that of bulk Y_2O_3 and close to that determined for Y-O clusters in as-synthesized nanoparticles (Table I). Thus, the MD simulation predicts a coordination environment of the surface yttrium atom that is consistent with the EXAFS data. In addition, the average Ti-O bond length in the simulation (1.9468 Å) is close to the experimental value for the as-synthesized nanoparticles (1.9538 Å).

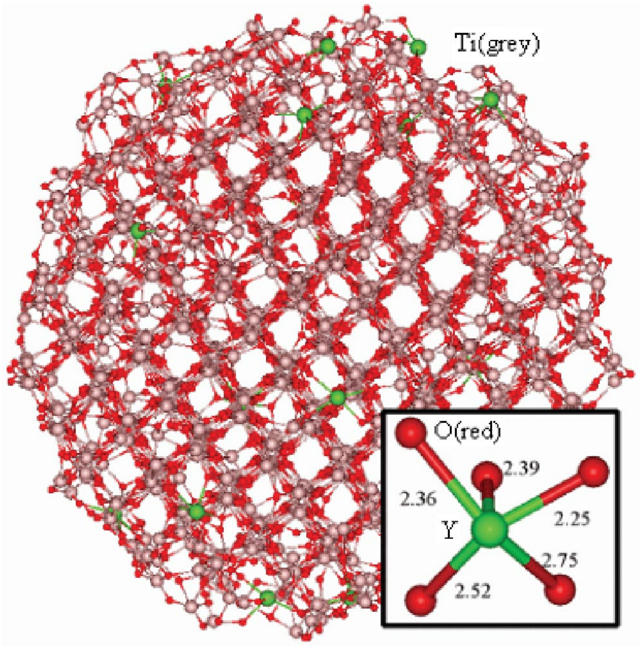

FIG. 1 (color). Distribution of Y atoms (green) at the surface of a 4 nm anatase particle given by a molecular dynamics simulation.

Regarding the elongation of the impurity Y-O bond relative to in bulk Y_2O_3, greater insight may be obtained with a simple electrostatic model. When Y-O ion pairs or clusters approach a particle surface closely enough ($\ll 100$ Å), polarization in the particle is induced. The interaction between the induced polarization charges and the ions in the Y-O clusters will depend on ionic charge, ion-surface distance, and surface curvature, thus providing a mechanism to alter the Y-O bond length. This can be mathematically described as the interaction of the Y-O cluster with its image in the particle [16]. Assuming the ions in the Y-O cluster possess their formal valence, and using the method of image for a Y-O bond that is perpendicular to the surface of a spherical TiO_2 particle of 6 nm in diameter, we estimate that an additional attraction force of 1.7 pN and repulsion force of 0.6 pN are exerted on Y^{3+} and O^{2-}, respectively. Because the ion in the dipole or multipole closest to the surface is attracted more than other ions, the Y-O bond will be elongated. The electric field close to the surface of a charged dielectric material is enhanced by curvature of the surface. Because heat treatment promotes coarsening and, hence, reduces surface curvature, the electric field near the surface and, thus, the cluster-particle interaction is reduced. This accounts for the shortening of the Y-O bond with increasing temperature of treatment.

To investigate the structural response of titania to the presence of impurities, we performed WAXS experiments on the samples. The results of pair distribution function refinement, through a fit with the PDFFIT code [17], are summarized in Table II, Fig. S2 in Ref. [12], and Figs. 2 and 3. The most notable results are that the presence of surface yttrium clusters inhibits both coarsening and the anatase-to-rutile transformation in nanocrystalline titania. For example, the diameters of anatase nanoparticles grew slowly from ~6 to ~10 nm over 2 h at 600 °C (Fig. 3). This strongly contrasts with the coarsening behavior of undoped anatase (anatase of ~6 nm grew to ~30 nm after annealing over 2 h at 525 °C [18]). Even more striking is the absence of the rutile phase below 600 °C, because undoped anatase nanoparticles start to transform to rutile at ~300 °C [6], and ~92% of nanocrystalline anatase transforms to rutile after 2 h treatment at 620 °C [19]. In fact, the phase analysis presented in Fig. 3 shows that the anatase-to-rutile transformation has been completely inhibited at all temperatures in the present system. At 600 °C and higher temperatures, rutile is formed at the expense of the brookite phase. The retardation of both particle growth and phase transformation is very desired for the catalytic applications of anatase, because coarsening and phase changes could result in the degradation of the catalytic properties of anatase [20]. A mechanistic insight into this unusual observation of retardation is obtained by detailed analysis of the trends in the structure of nanocrystalline titania with treatment temperature.

TABLE II. Fit results from WAXS data for Y-doped titania.

	T (°C)	Anatase				Brookite				
		Size (nm)	a (Å)	c (Å)	V (Å^3)	Size (nm)	a (Å)	b (Å)	c (Å)	V (Å^3)
Pure	20	Bulk [10]	3.785	9.514	136.30	Bulk [10]	9.184	5.447	5.145	257.38
	20	7.0(2)	3.786(1)	9.479(3)	135.87(44)	9.4(3)	9.149(10)	5.450(7)	5.179(6)	258.24(91)
Doped	20	6.0(2)	3.800(1)	9.509(4)	137.29(13)	5.4(1)	9.152(12)	5.447(8)	5.231(7)	260.77(107)
	300	6.0(2)	3.802(1)	9.490(4)	137.20(13)	5.4(1)	9.170(10)	5.448(6)	5.222(6)	260.88(87)
	400	6.4(2)	3.802(1)	9.496(4)	137.27(13)	5.7(2)	9.211(9)	5.441(6)	5.207(5)	260.96(79)
	500	9.6(3)	3.803(1)	9.498(4)	137.34(13)	6.3(2)	9.200(10)	5.437(6)	5.201(5)	260.16(81)
	600	9.3(3)	3.797(1)	9.516(4)	137.17(12)	7.6(3)	9.542(14)	5.270(8)	5.157(7)	259.33(113)
	700	14.3(3)	3.798(1)	9.529(3)	137.45(9)	9.7(3)	9.572(13)	5.282(7)	5.170(7)	261.39(106)

Our measurements show that the lattice parameters of undoped TiO_2 nanoparticles have no obvious changes with increasing treatment temperature in limited coarsening (from 7 to 10 nm) [19], but the presence of surface yttrium has a strong effect on the interior structure of the nanophase titania. We observed an expansion of the unit cell volumes of both anatase and brookite relative to the bulk and undoped nanocrystalline materials, at all temperatures up to 700 °C (Table II). Examinations of the detailed changes in unit cell parameters (Fig. 2) show that these structural changes are not isotropic but vary strongly with crystallographic orientation. For the anatase phase, the parameter c of the Y-doped samples is increased more than the parameter a relative to pure anatase nanoparticles. This is also seen in our MD simulations ($\Delta c = 0.0312$ Å, $\Delta a = -0.0036$ Å). These observations suggest that the cluster-particle interactions are not equivalent for the different crystallographic faces of the anatase nanoparticles. In particular, expansion of the d spacing normal to the anatase {001} face (equivalently, the c parameter) suggests a strong interaction at this face. Higher surface energy of {001} relative to {100} [21] suggests that its interactions with surface impurities are more thermodynamically favored. For the brookite phase, the effect of yttrium doping is to dramatically increase the unit cell c dimension relative to undoped nanoparticles of this phase, also suggesting a strong specific interaction with one face.

The strong suppression of growth permits the phase behavior to be interpreted using our understanding of phase stability inversions in nanosized titania [6,19]. In pure titania, it is estimated that anatase is the most thermodynamically stable phase at sizes less than ~11 nm, brookite between ~11 and ~35 nm, and rutile at greater than 35 nm

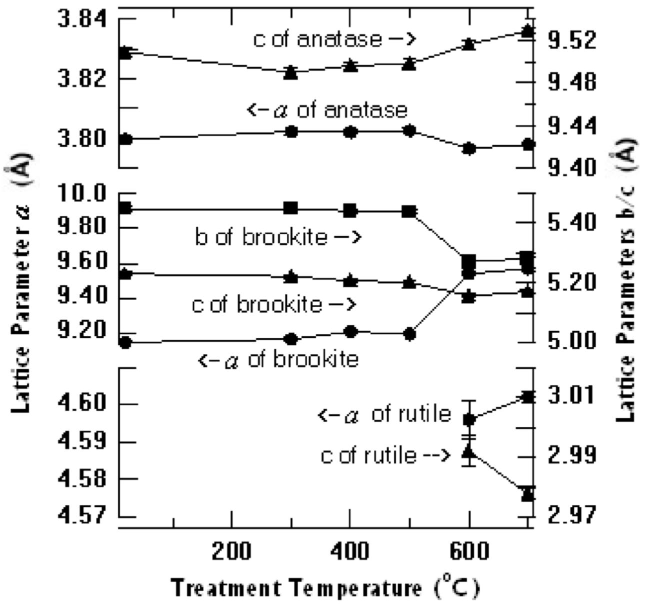

FIG. 2. Lattice parameters of anatase (top), brookite (middle), and rutile (bottom) as a function of treatment temperature.

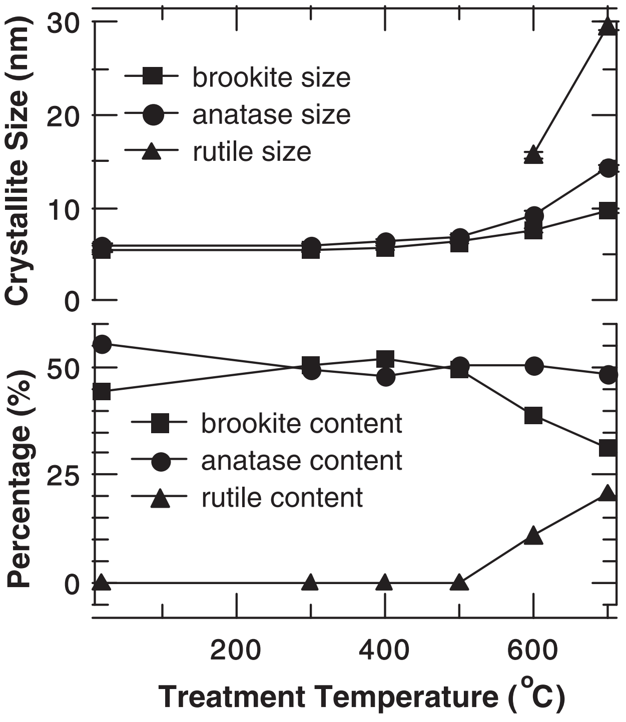

FIG. 3. Crystallite size as a function of treatment temperature (top). Percentage of constituent structures as a function of treatment temperature (bottom).

[19]. Thus, the dominant effect of yttrium is to inhibit coarsening, so that the anatase-to-rutile transformation is not thermodynamically favored. At the highest temperature (700 °C), the anatase particles grew to 14.3 nm but the crystalline structure is still unchanged, showing that surface interactions can retard phase transformation as well as growth. Because phase transformations in nanoparticles can be initiated through nucleation at interfaces between aggregated nanoparticles [19], surface dopants may stabilize phases by altering activation energy of transformation (a kinetic effect). However, because the phase relations determined for pure nanosized titania are likely altered in the presence of yttrium, the strong interactions at the anatase surfaces indicate that it might increase the stability regime of this phase with size (a thermodynamic effect).

We conclude that the key factor in the observed structural modification and retardation behavior is that surface yttrium lowers the interfacial free energy of one or more surfaces of nanoscale TiO_2. Surface adsorption generally lowers substrate surface energy, and this is confirmed for the present system by MD simulation. The surface energy of the Y-doped anatase nanoparticle is estimated to be $0.94\ J/m^2$, much lower than the value for undoped 4 nm anatase calculated by the same method ($2.1\ J/m^2$, Ref. [22]). Comparison of the lattice energy of $YO_{3/2}$ (6353.5 kJ/mol) and TiO_2 (12 150 kJ/mol) also predicts a lower surface energy for faces terminated by yttrium vs. titanium sites coordinated by 6 oxygen atoms [23].

In summary, we have shown that the low concentrations of impurity ions that are not incorporated into the interiors of TiO_2 nanoparticles reduce surface energy and inhibit nanoparticle growth over a large temperature range. As a consequence, the anatase phase is also stabilized, as the anatase-to-rutile transformation does not occur below 700 °C. Our findings demonstrate the effectiveness of surface bound impurities of stabilizing nanoparticle size and phase, an issue of great importance for retaining the materials properties of nanoscale catalysts that operate at high temperatures.

We thank Brian Lee Bischoff for the synthesis of raw materials and Dr. Michael Kruger and Dr. Glenn Waychunas for helpful discussions. We thank Matthew Latimer, Allyson Aranda, John Bargar, and Joe Rogers for help with EXAFS measurements on beam lines 10-2/11-2, SSRL, and Ren Yang and Steven Weigand for help with WAXS measurements on beam lines 11-ID-C/5-ID-D, APS, Argonne National Laboratory. Use of APS was supported by the U.S. Department of Energy, Office of Science, Office of Basic Energy Sciences, under Contracts No. DE-AC02-06CH11357 and No. W-31-109-Eng-38. Financial support for this work was provided by the U.S. Department of Energy (Grants No. DE-FG03-01ER15218 and DE-AC02-05CH11231) and the National Science Foundation (Grant No. EAR-0123967).

---

*To whom all correspondence should be addressed. Electronic address: binchen@berkeley.edu

[1] K. Hund-Rinke and M. Simon, Environ. Sci. Pollut. Res. Int. **13**, 225 (2006).
[2] B. O'Reganand and M. Grätzel, Nature (London) **353**, 737 (1991).
[3] A. Fuerte *et al.*, Chem. Commun. (Cambridge) **24**, 2718 (2001).
[4] H. Zhang *et al.*, Nature (London) **424**, 1025 (2003).
[5] F. Huang *et al.*, Phys. Rev. Lett. **92**, 155501 (2004).
[6] J. F. Banfield, B. L. Bischoff, and M. A. Anderson, Chem. Geol. **110**, 211 (1993).
[7] B.L. Bischoff, Ph.D. dissertation, University of Wisconsin–Madison, 1992.
[8] Y. H. Zhang and A. Reller, J. Mater. Chem. **11**, 2537 (2001).
[9] H. Yamashita *et al.*, J. Synchrotron Radiat. **6**, 451 (1999).
[10] G. V. Samsonov, *The Oxide Handbook* (IFI/Plenum, New York, 1982).
[11] M. A. Anderson, M. J. Gieselmann, and Q. Xu, J. Membr. Sci. **39**, 243 (1988).
[12] See EPAPS Document No. E-PRLTAO-98-080710 for (a) an estimation of yttrium surface site coverage, (b) MD simulation, (c) Fig. S1—EXAFS spectra and the first-shell fit, and (d) Fig. S2—the PDF fit of the WAXS data. For more information on EPAPS, see http://www.aip.org/pubservs/epaps.html.
[13] F. D. Bloss, *Crystallography and Crystal Chemistry* (Holt, Rinehart and Winston, New York, 1971).
[14] L. X. Chen *et al.*, J. Phys. Chem. B **101**, 10 688 (1997).
[15] N. Thromat *et al.*, Phys. Rev. B **44**, 7904 (1991).
[16] J. D. Jackson, *Classical Electrodynamics* (Wiley, New York, 1990).
[17] T. Proffen *et al.*, J. Appl. Crystallogr. **32**, 572 (1999).
[18] A. A. Gribb and J. F. Banfield, Am. Mineral. **82**, 717 (1997).
[19] H. Zhang and J. F. Banfield (unpublished); J. Mater. Res. **15**, 437 (2000); J. Phys. Chem. B **104**, 3481 (2000); J. Mater. Chem. **8**, 2073 (1998).
[20] K. I. Hadjiivanov and D. G. Klissurki, Chem. Soc. Rev. **25**, 61 (1996).
[21] M. Lazzeri *et al.*, Phys. Rev. B **63**, 155409 (2001).
[22] P. K. Naicker *et al.*, J. Phys. Chem. B **109**, 15 243 (2005).
[23] *CRC Handbook of Chemistry and Physics*, edited by D. R. Lide (Internet version 2007), 87th ed.